MIT Libraries | DSpace@MIT

MIT Open Access Articles

Adjoint-Based Sensitivity Analysis for Silicon Photonic Variations

The MIT Faculty has made this article openly available. ***Please share*** how this access benefits you. Your story matters.

Citation: Zhengxing, Zhang et al. "Adjoint-Based Sensitivity Analysis for Silicon Photonic Variations." 2019 IEEE MTT-S International Conference on Numerical Electromagnetic and Multiphysics Modeling and Optimization, May 2019, Boston, MA, Institute of Electrical and Electronics Engineers, October 2019. © 2019 IEEE

As Published: http://dx.doi.org/10.1109/nemo.2019.8853679

Publisher: Institute of Electrical and Electronics Engineers (IEEE)

Persistent URL: https://hdl.handle.net/1721.1/130927

Version: Author's final manuscript: final author's manuscript post peer review, without publisher's formatting or copy editing

Terms of use: Creative Commons Attribution-Noncommercial-Share Alike

Massachusetts Institute of Technology

Adjoint-Based Sensitivity Analysis for Silicon Photonic Variations

Zhengxing Zhang, Sally I. El-Henawy, Allan Sadun, Ryan Miller, Luca Daniel, Jacob K. White, and Duane S. Boning

***Abstract*—With the rising demand for integrated silicon photonics as a technology platform, it becomes crucial to provide variation-aware models and design for manufacturability (DFM) methods to inform the design of silicon photonic devices and circuits. In this paper, we demonstrate the application of the adjoint method to estimating the sensitivity of photonic components against key process variations inherited from integrated circuit fabrication technologies. In particular, we examine the impact of line edge roughness (LER) on a passive Y-branch, and validate our results with ensemble virtual fabrication simulations. The adjoint sensitivity and variance estimation of Y-branch transmission imbalance is seen to be highly efficient in comparison to direct ensemble simulation.**

***Index Terms*—Silicon photonics, process variations, line edge roughness, adjoint method, DFM, Y-branch, sensitivity analysis**

I. INTRODUCTION

As a promising technology platform for various applications [1]–[4], silicon photonics now needs mature variation-aware models and methods for manufacturing design. To be cost-effective, the field of silicon photonics leverages the existing IC manufacturing infrastructure for fabricating photonic components. This means, however, that the process variations experienced in IC fabrication are also present in silicon photonics.

Unlike in conventional ICs, the effect of process variations in silicon photonics has seen relatively limited consideration in the literature [5]–[8]. Methods to understand the impact of such variations on fundamental silicon photonic devices and components are necessary to achieve high-yield photonic integrated circuits (PICs).

In this paper, we further develop the adjoint method [9], [10] in order to enable sensitivity analysis for silicon photonic components. In particular, we show as an example how it can be used to assess the effects of line edge roughness on the transmission coefficient in a Y-branch. We finally validate our results with ensemble virtual fabrication simulations.

II. TECHNICAL BACKGROUND

Given a linear and reciprocal system, the adjoint (or adjoint state) method in its original form [11] is a numerical method that allows the efficient computation of the sensitivity (i.e., gradient) of the system performance merit function $F(\cdot)$ with respect to the system parameters. Acceleration of the sensitivity evaluation of a merit function is critical in problems that require a large number of such evaluations, such as in design optimization [10]. A simple finite difference sensitivity approach typically requires $O(P)$ system solves, where P is the number of parameters. In comparison, adjoint sensitivity does not depend on P, and typically requires $O(M)$ system solves, where M is the number of output quantities of interest that contribute to the merit function. Therefore the adjoint method is particularly useful in problems where the number of parameters is much larger than the number of output quantities of interest, $P \gg M$.

In computational electromagnetics and photonics, the adjoint method was first used in [9] and is now being further employed for shape optimization and inverse design [10]. In those settings the merit function was in the form of a real-valued function,

$$F(\varepsilon(\mathbf{x})) = \int_\chi f\left[\mathbf{E}(\mathbf{x};\varepsilon(\mathbf{x})), \mathbf{H}(\mathbf{x};\varepsilon(\mathbf{x}))\right] \, \mathrm{d}^3\mathbf{x}, \tag{1}$$

where χ is the "evaluation" region over which the fields are to be optimized. Then the adjoint method gives the variation δF caused by an infinitesimal change $\delta\varepsilon(\mathbf{x})$ in the permittivity parameters of some region ψ of the medium

$$\delta F = 2\,\mathrm{Re} \int_\psi \delta\varepsilon(\mathbf{x}') \; \mathbf{E}(\mathbf{x}';\varepsilon(\mathbf{x})) \cdot \mathbf{E}^A(\mathbf{x}';\varepsilon(\mathbf{x})) \, \mathrm{d}^3\mathbf{x}', \tag{2}$$

$$\mathbf{E}^A(\mathbf{x}';\varepsilon(\mathbf{x})) = \int_\chi \left[G^{\mathrm{EP}}(\mathbf{x}';\mathbf{x}) \frac{\partial f}{\partial \mathbf{E}} - G^{\mathrm{EM}}(\mathbf{x}';\mathbf{x}) \frac{\partial f}{\partial \mathbf{H}} \right] \mathrm{d}^3\mathbf{x} \tag{3}$$

where (3) is the electric field from the adjoint simulation, using dipole sources $(\mathbf{P}, \mathbf{M}) = \left(\frac{\partial f}{\partial \mathbf{E}}, -(1/\mu_0) \frac{\partial f}{\partial \mathbf{H}} \right)$ in the region χ.

III. THE ADJOINT METHOD FOR S-PARAMETERS OF SILICON PHOTONIC DEVICES

In this section, we discuss the use of the adjoint method for silicon photonic devices and we further extend it to include also estimation of merit function variance. For silicon photonic devices, the merit functions we are often interested in are the complex-valued optical S-parameters [1], $F(\cdot) = S_{12}$, defined using mode expansion coefficients in [12]. Conveniently, following the same path as in [9] and applying equivalent source theory [13] to convert the dipole sources to mode sources, we find that the adjoint simulation for variation in S_{12} is just the reciprocal simulation used to find S_{21}.

If we denote the source mode expansion coefficient in port 1, the monitor mode expansion coefficient in port 2, and

Zhengxing Zhang (zhxzhang@mit.edu), Sally I. El-Henawy, (elhenawy@mit.edu), Allan Sadun (sadun@mit.edu), Luca Daniel (luca@mit.edu), Jacob K. White (white@mit.edu), and Duane S. Boning (boning@mtl.mit.edu) are with the Massachusetts Institute of Technology. Ryan Miller (rmiller@coventor.com) is with Coventor Inc.

the electrical field in the S_{12} simulation as s_1, a_{12}, and $\mathbf{E}_1$, respectively; the terms s_2, a_{21}, and $\mathbf{E}_2$ analogously for S_{21}; and the power of the mode in port 1 and port 2 as N_1 and N_2, then from [12],

$$S_{12} = \frac{a_{12}\sqrt{N_2}}{s_1\sqrt{N_1}}, \qquad S_{21} = \frac{a_{21}\sqrt{N_1}}{s_2\sqrt{N_2}} \tag{4}$$

and $S_{12} = S_{21}$ by the reciprocity of S-parameters. Adjoint method theory then gives

$$\begin{aligned} \delta S_{12} &= \delta S_{21} \\ &= \frac{\mathrm{i}\pi f}{2 s_1 s_2 \sqrt{N_1 N_2}} \int_\psi \delta\varepsilon(\mathbf{x}')\mathbf{E}_1(\mathbf{x}') \cdot \mathbf{E}_2(\mathbf{x}')\, \mathrm{d}^3\mathbf{x}' \end{aligned} \tag{5}$$

In general, the output variation δF in the adjoint method can be written in the form

$$\delta F = \int_\psi R(\mathbf{x}')\delta n(\mathbf{x}')\, \mathrm{d}^3\mathbf{x}', \tag{6}$$

where $\delta n(\mathbf{x})$ is the refractive index variation (assumed here to be real), and $R(\mathrm{x}')$ is the refractive index sensitivity function which is connected with the inner product of the electrical fields. Thus the mean and variance of the output variation can be estimated by

$$\langle \delta F \rangle \approx \int_\psi R(\mathbf{x}')\langle \delta n(\mathbf{x}')\rangle\, \mathrm{d}^3\mathbf{x}', \tag{7}$$

$$\langle (\delta F)^2 \rangle \approx \int_\psi \int_\psi R(\mathbf{x}')R(\mathbf{x}'')\langle \delta n(\mathbf{x}')\delta n(\mathbf{x}'')\rangle\, \mathrm{d}^3\mathbf{x}'\mathrm{d}^3\mathbf{x}'', \tag{8}$$

which can be numerically calculated for any given refractive index variation.

IV. Implementation: LER on Y-Branch

In this section, we implement the adjoint method analysis for a fundamental photonic component present in almost all photonic integrated circuits, a silicon-on-insulator (SOI) Y-branch. The geometry of the Y-branch used here is similar to that presented in [14], with a nominal waveguide width of 500 nm, length of 15 μm and thickness of 220 nm. The two parameters that characterize the LER are its root mean square amplitude A and correlation length L_c as in (9):

$$N = A^2 e^{-(x/L_c)^2} \tag{9}$$

where x is the distance along the length of the structure. One instantiation of a Y-branch with LER as generated by the SEMulator3D® [15] software is shown in Fig. 1. We seek to estimate the mean and variance of transmission power imbalance caused by LER.

The input port is labeled as port 1, and the two output ports are labeled as port 2 and 3. From (4) and (5), the variation of the output transmission power is

$$\delta T_i = -\frac{\pi f}{|s_1|^2 N_1} \mathrm{Im}\, \frac{a_{1i}^*}{s_i} \int_\psi \delta\varepsilon(\mathbf{x}')\mathbf{E}_1(\mathbf{x}') \cdot \mathbf{E}_i(\mathbf{x}')\, \mathrm{d}^3\mathbf{x}' \tag{10}$$

for $i = 2, 3$. Since we have symmetry $a_{12} = a_{13}$, $s_2 = s_3$, the

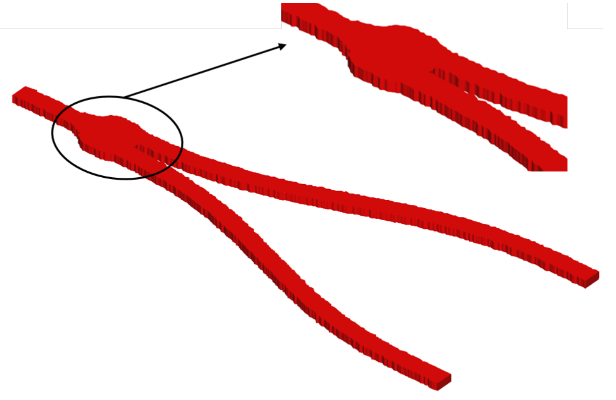

Fig. 1. Y-branch geometry with LER ($A = 12$ nm and $L_c = 50$ nm).

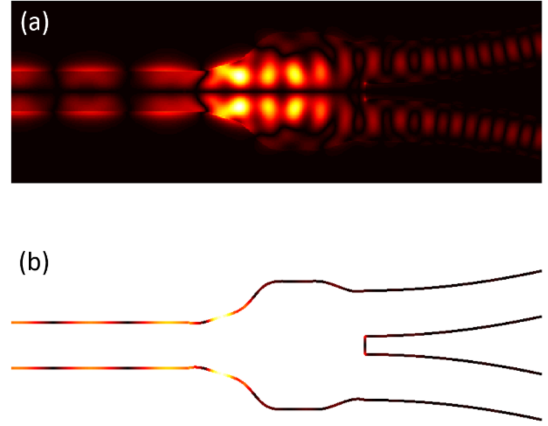

Fig. 2. Adjoint method analysis results: (a) absolute value of refractive index sensitivity function $|R(\mathbf{x}')|$, plane view; (b) absolute value of geometry sensitivity function $|g(x', y')|$ on the sidewall contour.

transmission power imbalance is thus

$$\delta T = \delta T_2 - \delta T_3 = \int_\psi R(\mathbf{x}')\delta n(\mathbf{x}')\, \mathrm{d}^3\mathbf{x}', \tag{11}$$

where the refractive index sensitivity function is

$$R(\mathbf{x}') = -\frac{2\pi f \varepsilon_0}{|s_1|^2 N_1} \mathrm{Im}\, \frac{a_{12}^*}{s_2} n(\mathbf{x}')\mathbf{E}_1(\mathbf{x}') \cdot [\mathbf{E}_2(\mathbf{x}') - \mathbf{E}_3(\mathbf{x}')] \tag{12}$$

and ε_0 is the vacuum permittivity. Fig. 2(a) shows the plane view of $|R(\mathbf{x}')|$.

However, the LER problem involves geometry variation on the sidewall, not just a simple refractive index variation. Moreover, the electrical field is not even continuous at the interface. Ref. [16] provides the solution to the boundary perturbation problem by rewriting the integral in (4) in terms of the parallel component of electric field $E_\parallel$ and the perpendicular component of electric displacement field $D_\perp$, which are continuous at the material interface. Then we can rewrite

(11) and (12) as

$$\delta T = \int_C g(x', y') \delta x'_n \, \mathrm{d}l', \tag{13}$$

where the integral is performed on the sidewall contour C, δx_n is the surface variation in the normal direction, and the geometry sensitivity function is

$$g(x', y') = -\frac{\pi f \varepsilon_0}{|s_1|^2 N_1} \mathrm{Im}\, \frac{a_{12}^*}{s_2} \int_0^h \Big[\Delta(n^2) \left(E_{1\parallel} \cdot E_{\parallel}^A \right) - \Delta(n^{-2}) \left(D_{1\perp} \cdot D_{\perp}^A \right) / \varepsilon_0^2 \Big] \, \mathrm{d}z', \tag{14}$$

where the adjoint field $\mathbf{E^A} = \mathbf{E_2} - \mathbf{E_3}$, $\mathbf{D^A} = \mathbf{D_2} - \mathbf{D_3}$, and $\Delta(n^d) = n_1^d - n_2^d$ is the d-th power index difference between silicon and the oxide cladding.

Fig. 2(b) plots $|g(x', y')|$ on the sidewall. The variance of the imbalance can now be computed from (13) and (9) as

$$\langle (\delta T)^2 \rangle \approx A^2 \int_C \int_C g(x', y') g(x'', y'') e^{-\left(|\mathbf{x}' - \mathbf{x}''|/L_c\right)^2} \, \mathrm{d}l' \mathrm{d}l''. \tag{15}$$

When the correlation length L_c is much smaller than the length scale at which $g(x', y')$ varies, (15) can be approximated and simplified as

$$\langle (\delta T)^2 \rangle \approx \sqrt{\pi} A^2 L_c \int_C g^2(x', y') \, \mathrm{d}l'. \tag{16}$$

All of the S-parameter coefficients including s_i, a_i, and N_i, and the electrical field $\mathbf{E}_i$ are easily acquired from an S-parameter sweep using the Lumerical FDTD 3D simulator [17] or varFDTD 2.5D simulator [18]. The computational time for a single simulation in FDTD 3D of the Y-branch with the highest mesh accuracy setting is approximately 40 minutes on an Intel(R) Xeon(R) CPU E7-4850 v4 @ 2.10GHz system. Due to the component symmetry, $\mathbf{E}_3$ can be acquired from $\mathbf{E}_2$, thus the whole process can be completed in under 80 minutes. One limitation is the memory cost for the storage of the electrical field, which is around 1.5 GB for a single wavelength in FDTD 3D simulation; thus the analysis can only be performed at a limited number of frequency points. Implementation in the varFDTD 2.5D simulator can reduce both computational time and memory requirement, but at the cost of lower accuracy.

V. Ensemble Simulations and Validation

In this section we use ensemble virtual fabrication simulations to verify the results from the adjoint method. More specifically, we virtually fabricate the Y-branch by modeling lithography (with LER) and etch process steps forming the SOI waveguide using SEMulator3D [15]; the output structure is shown in Fig. 1. The LER is defined as Gaussian noise using a Fourier synthesis technique [19], [20] and then imposed on the Y-branch as geometric sidewall perturbations. The structures are then exported from SEMulator3D and imported into Lumerical FDTD [17] for optical simulation.

Previous work [8] has shown that LER causes transmission imbalance between the two Y-branch output ports, and the degree of imbalance depends on the particular instantiation of LER. Since LER is a random variable, running an ensemble of 50 different instantiations for each A and L_c combination we are examining enables us to identify the mean and variance of the transmission imbalance resulting from LER.

TABLE I
Comparison of standard deviation of transmission power imbalance at operating wavelength ($\lambda = 1550$ nm) where σ_1, σ_2 and σ_3 are the standard deviation for virtual fabrication, adjoint method from 3D simulations, and adjoint method from 2.5D simulations, respectively.

A (nm)	L_c (nm)	σ_1 ($\times 100$)	σ_2 ($\times 100$)	σ_3 ($\times 100$)
1	25	0.2497	0.3065	0.3470
3	10	0.4512	0.5833	0.6585
3	20	0.6367	0.8234	0.9312
3	40	0.9024	1.1578	1.3169
6	60	2.7097	2.8130	3.2258
7	30	2.3283	2.3471	2.6612
10	10	1.8569	1.9444	2.1949
10	40	3.8494	3.8595	4.3898
12	50	4.0369	5.1583	5.8895
15	60	5.6474	7.0325	8.0646

Table I shows the standard deviation of transmission power imbalance ($\sigma = \sqrt{\langle (\delta T)^2 \rangle}$), as computed by ensemble simulations (σ_1), by the adjoint method (14, 15) implemented with 3D simulation (σ_2), and by the adjoint method implemented with 2.5D simulation (σ_3) for the different amplitude/correlation length combinations of LER applied to the Y-branch, all at an operating wavelength of 1550 nm.

For LER amplitude $6 \text{ nm} \leq A \leq 10 \text{ nm}$, the differences between the adjoint method (σ_2) and ensemble simulations (σ_1) are very small. Considering the potential error in σ_1 which estimates variance from only 50 random samples, adjoint method results are seen to have sufficient accuracy. However, the difference increases to over 20% for both small and large A. It is likely that the FDTD grid has difficulty in capturing the details of small amplitude LER; thus ensemble simulations are likely giving less accurate results for the small amplitude region and the adjoint method may be superior for handling such small variations. However, for the large A LER cases, the first order approximation used in the adjoint method begins to hit the limits of the approximation and give less accurate results. We see that the adjoint method using the 2.5D simulator always gives less accurate, but still reasonable results, compared to the adjoint method with FDTD 3D simulations.

An important limitation is also present when using the adjoint method alone. In some cases, in addition to the (differential) sensitivity to variation, we are concerned with mean shifts resulting from the variation. Fig. 3 compares the distribution of transmission powers of the two output ports, based on ensemble simulations and adjoint method prediction. We see that the mean of the scatter of ensemble simulation

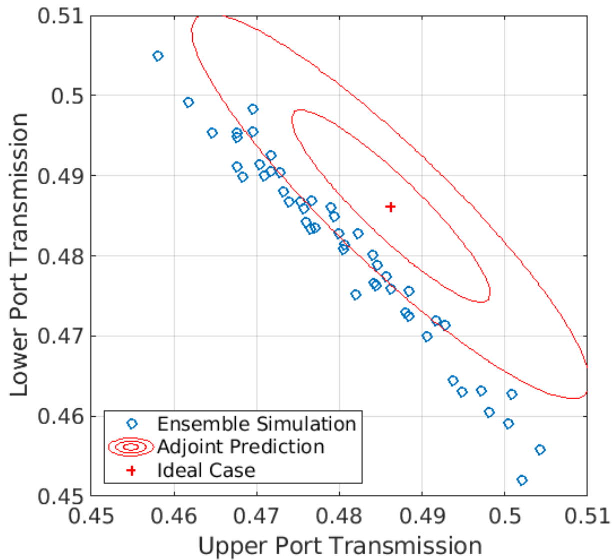

Fig. 3. Comparison between the scatter of transmission values of the ensemble simulations (blue circles) with the distribution predicted by the adjoint method (red line, 1σ and 2σ boundaries are shown) at LER variation $A = 7$ nm and $L_c = 30$ nm.

outputs are shifted from the center of the adjoint prediction. This is because the adjoint method ignores the scatter field loss caused by LER which shifts the mean of output power distribution to below the ideal case having no LER.

VI. Conclusion

We have presented a methodology to perform efficient sensitivity analysis on silicon photonic devices using the adjoint method. The methodology can be applied to many device components and different types of process variation. In this work we have demonstrated its validity and efficiency when determining the sensitivity of the transmission coefficients in Y-branches against line edge roughness (LER) process variations.

In particular, we have shown that for small variations in LER, the adjoint method can estimate with good or potentially better accuracy the variance of our merit function in 80 minutes for any given input variation (value of LER amplitude A and correlation length L_c), compared to 100 hours required by ensemble virtual fabrication simulations (i.e., 50 virtual fabrication and FDTD simulations each requiring 2 hours) for each A and L_c combination. The computational time and memory cost can be further reduced using varFDTD 2.5D simulations if a 15% error can be tolerated. We have also observed that the adjoint method starts to fail for A larger than 10 nm, and that it ignores the scatter loss caused by LER. The number of frequency points that can be examined in the adjoint method is largely limited by the computational memory cost.

Further work could explore a hybrid approach that takes advantage of the strengths of each analysis method. For example, for LER with small amplitude, the adjoint method combined with a smaller number of ensemble simulations could potentially capture both mean shift effects and accurate statistical sensitivities, much more efficiently and accurately than using either method alone.

Acknowledgment

This material is based on research sponsored in part by AIM Photonics and Air Force Research Laboratory under agreement number FA8650-15-2-5220. The U.S. Government is authorized to reproduce and distribute reprints for Governmental purposes notwithstanding any copyright notation thereon. The views and conclusions contained herein are those of the authors and should not be interpreted as necessarily representing the official policies or endorsements, either expressed or implied, of Air Force Research Laboratory or the U.S. Government.

References

[1] L. Chrostowski and M. Hochberg, *Silicon Photonics Design: From Devices to Systems*. Cambridge University Press, 2015.
[2] X. Wang, W. Shi, H. Yun, S. Grist, N. A. Jaeger, and L. Chrostowski, “Narrow-band waveguide Bragg gratings on SOI wafers with CMOS-compatible fabrication process,” *Optics Express*, vol. 20, no. 14, pp. 15 547–15 558, 2012.
[3] C. Sun, M. T. Wade, Y. Lee, J. S. Orcutt, L. Alloatti, M. S. Georgas, A. S. Waterman, J. M. Shainline, R. R. Avizienis, S. Lin *et al.*, “Single-chip microprocessor that communicates directly using light,” *Nature*, vol. 528, no. 7583, p. 534, 2015.
[4] J. E. Bowers, T. Komljenovic, M. Davenport, J. Hulme, A. Y. Liu, C. T. Santis, A. Spott, S. Srinivasan, E. J. Stanton, and C. Zhang, “Recent advances in silicon photonic integrated circuits,” in *Next-Generation Optical Communication: Components, Sub-Systems, and Systems V*, vol. 9774. International Society for Optics and Photonics, 2016, p. 977402.
[5] R. Wu, C.-H. Chen, T.-C. Huang, R. Beausoleil, and K.-T. Cheng, “Spatial pattern analysis of process variations in silicon microring modulators,” in *IEEE Optical Interconnects Conf.*, 2016, pp. 116–117.
[6] D. Melati, A. Melloni, and F. Morichetti, “Real photonic waveguides: guiding light through imperfections,” *Advances in Optics and Photonics*, vol. 6, no. 2, pp. 156–224, 2014.
[7] W. A. Zortman, D. C. Trotter, and M. R. Watts, “Silicon photonics manufacturing,” *Optics Express*, vol. 18, no. 23, p. 23598, 2010.
[8] S. I. El-Henawy, R. Miller, and D. S. Boning, “Effects of a random process variation on the transfer characteristics of a fundamental photonic integrated circuit component,” in *Proc. of SPIE*, vol. 10743, 2018, pp. 107 430O–1–107 430O–10.
[9] O. D. Miller, “Photonic design: From fundamental solar cell physics to computational inverse design,” *preprint arXiv:1308.0212*, 2013.
[10] C. M. Lalau-Keraly, S. Bhargava, O. D. Miller, and E. Yablonovitch, “Adjoint shape optimization applied to electromagnetic design,” *Optics Express*, vol. 21, no. 18, p. 21693, 2013.
[11] F. Branin, “Network sensitivity and noise analysis simplified,” *IEEE Trans. on Circuit Theory*, vol. 20, no. 3, pp. 285–288, 1973.
[12] A. W. Snyder and J. D. Love, *Optical Waveguide Theory*. Boston, MA: Springer, 1984.
[13] A. Oskooi and S. G. Johnson, “Electromagnetic Wave Source Conditions,” *preprint arXiv:1301.5366*, 2013.
[14] Y. Zhang, S. Yang, A. E.-J. Lim, G.-Q. Lo, C. Galland, T. Baehr-Jones, and M. Hochberg, “A compact and low loss Y-junction for submicron silicon waveguide,” *Optics Express*, vol. 21, no. 1, pp. 1310–1316, 2013.
[15] SEMulator3D 7.1, Coventor Inc. [Online]. Available: https://www.coventor.com/semiconductor-solutions/semulator3d
[16] S. G. Johnson, M. Ibanescu, M. A. Skorobogatiy, O. Weisberg, J. D. Joannopoulos, and Y. Fink, “Perturbation theory for Maxwell’s equations with shifting material boundaries,” *Phys. Rev. E*, vol. 65, p. 066611, June 2002.
[17] [Online]. Available: https://www.lumerical.com/products/fdtd-solutions
[18] [Online]. Available: https://www.lumerical.com/products/mode-solutions
[19] C. A. Mack, “Generating random rough edges, surfaces, and volumes,” *Applied Optics*, vol. 52, no. 7, pp. 1472–1480, 2013.
[20] A. Asenov, S. Kaya, and A. R. Brown, “Intrinsic parameter fluctuations in decananometer MOSFETs introduced by gate line edge roughness,” *IEEE Trans. on Electron Devices*, vol. 50, no. 5, pp. 1254–1260, 2003.